

Graphene based porous magnetic aerogel powder for removal of methylene blue from waste water

Rahul Sharma,^{1,2} R.K. Kotnala,¹ Parveen Saini^{1*}

¹ CSIR-National Physical Laboratory, New Delhi-110012, INDIA

² Academy of Scientific & Innovative Research (AcSIR), New Delhi-110012, INDIA

ORIGINAL RESEARCH ARTICLE

ABSTRACT

Graphene based porous magnetic aerogel powder (MAP) has been prepared by facile and scalable route involving hydrothermal treatment of graphene oxide (GO) dispersion containing magnetite (Fe_3O_4) nanoparticles followed by freeze drying. The formed MAP is demonstrated as an efficient adsorbent material for methylene blue (MB) dyes present in water as a deliberately added impurity. The presence of Fe_3O_4 phase checks the agglomerating tendency of in-situ reduced GO (RGO) layers, simultaneously imparting magnetic character. The high porosity of MAP allowed rapid adsorption of MB molecules from water whereas coupled magnetic character enabled easy magnetic separation of dye sorbed MAP particles from purified water. The system was found to rapidly (in 30 s) decolorize the MB containing water with instantaneous adsorption capacity of 130 mg/g. The adsorption mechanism involves ultrafast electrostatic interactions between cationic dye molecules and electron density rich oxygen functional groups present on MAP surfaces.

KEYWORDS

adsorption; graphene oxide; methylene blue; porous composites; reduced graphene oxide

1. INTRODUCTION

The contamination of water resources by effluents of leather, paper and textile industries containing huge amounts of synthetic dyes is a major concern worldwide. Besides their adverse effects on human beings, being deeply coloured and multi component; dyes inhibit self purification of water, consume dissolved oxygen and destroy aquatic life (Sharma and Saini, 2016; Mukherjee et al., 2015; Shannon et al., 2008; Sulak and Yatmaz, 2012; Rafatullah et al., 2010). Among various waste water treatment approaches (Khin et al., 2012; Jiao et al., 2015) adsorption is considered as most simple, economical and viable process. In this context, numerous adsorbent materials such as activated carbon (Namasivayam and Kavitha, 2002; Dias et al., 2007; Ai et al., 2011), natural materials (Tan, 2000), bio adsorbents and agriculture waste (Muthuraman et al., 2009; Bhatnagar and Sillanpää,

2010) products have been explored for such processes on the basis of their physicochemical properties. However, these conventional adsorbents suffer from poor adsorption capacity, non recyclability and sometimes high cost of production. In recent past, nanoscience has been emerging with the development of new novel technologies and nanomaterials which showed promising potential in enormous applications among which waste water treatment is extensively examined (Pradeep and Anshup, 2009; Prado and Costa, 2009; Ambashta and Sillanpää, 2010; Tripathi et al., 2013; Khan et al., 2016; Saini et al., 2016a and b). Particularly, carbon based nanomaterials due to their simplicity, biocompatibility and easy scalable synthetic routes have become the earmark adsorbents (Sharma and Saini, 2016; Saini et al., 2016a). Interestingly, graphene owing to its very large specific surface area $2630 \text{ m}^2/\text{g}$, extraordinary properties and environmental friendliness has become the most

Corresponding author: P. Saini

Tel: +91-11-45609505/45608627

Fax: +91-11-45609301

E. mail: pksaini@nplindia.org; parveensaini580@gmail.com

Received: 10-11-2016

Revised: 22-11-2016

Accepted: 14-12-2016

Available online: 01-01-2017

extensively studied material in current times (Sharma and Saini, 2016). However, inherent hydrophobicity and agglomerating tendency of graphene 2D sheets restricts their potential in adsorption based wastewater treatment applications. Further, recontamination evading of water phases by graphene based nano size adsorbent particles is a challenging issue and therefore, facile and complete recovery of sorbed material is highly desirable. In this context, magnetic adsorbents such as Fe_3O_4 exhibit unique advantage due to their quick and effective magnetic separation. However, adsorption capacities of such materials are quite poor as agglomeration of nanoparticles significantly reduce the surface area of adsorbent. Therefore, it was expected that merging of characteristics of both graphene 2D sheets and magnetic Fe_3O_4 nanoparticles impart magnetic character in the adsorbent and simultaneously reduce the agglomerating tendency of each other. Interestingly, in recent past graphene oxide (GO) because of its unique physicochemical characteristics, has emerged as scaffold material for synthesis of graphene based macroscopic hydrogel and aerogel materials. These materials are well known for interesting features such as ultra light weight, high porosity and large surface area.

The aim of the work is to fabricate a light weight, low density, highly porous graphene based aerogel powder adsorbent possessing magnetic character for the efficient and effective removal of cationic dye MB from its aqueous solutions. Also, to exploit the aqueous phase process characteristics of GO sheets for construction of ethylenediamine mediated 3D interconnected porous network with simultaneous coupling of magnetic magnetite nanoparticles. The novel 'sol-gel' and subsequent "freeze-drying" strategy is employed in the present study for synthesis of magnetic aerogel powder (MAP) adsorbent. The synthesised MAP is expected to exhibit promising dye removal efficiency and easy recoverability from water phase.

2. MATERIALS AND METHODS

2.1. Materials

Graphene oxide (GO) was prepared using modified Hummers method (Hummers and Offeman, 1958) using natural graphite. In a typical procedure 3 g powdered graphite was added to the mixture of sulphuric acid (70 mL, 98% MERCK) and sodium nitrate (3 g, MERCK). After mixing the graphite uniformly, potassium

permanganate (9 g, MERCK) was added very slowly to the reaction mixture at ice bath keeping temperature below 20 °C. After 18 h of stirring, a purple paste was formed which was diluted by 140 mL of distilled water. The color of mixture changed to brown with brisk effervescences during addition of water and the temperature of reaction mixture also increased to 98 °C. After 20 min of stirring, the brown color mixture was further diluted with 440 mL of distilled water followed by addition of hydrogen peroxide (20 mL, 30%, MERCK). Finally, the colour of mixture was changed to bright yellow. The yellow colour product was filtered off and washed several times with 2% hydrochloric acid (prepared from 37% hydrochloric acid, MERCK) followed by warm water to remove the salt and acidic impurities. The neutral brown product then dried at 45 °C in vacuum oven to get the graphene oxide (GO) flakes.

2.2. Synthesis of MAP

To 10 mL GO aqueous dispersion (3 mg/mL) in a glass vial, 20 mg of Fe_3O_4 (Sigma Aldrich, <50 nm) nanoparticles were added. The mixture was stirred for 10 min followed by addition of 30 μL ethylenediamine (MERCK, 99%). After proper mixing the components, glass vial was heated at 95 °C for 6 h (Figure 1a displays the schematic representation of (MAP) synthesis). The resulted gel like product was then freeze dried to obtain the graphene based MAP.

2.3. Characterization

The obtained GO and MAP samples were characterized by Fourier Transform Infrared spectroscopy, FTIR (Cary 630 model, Agilent technologies), X-Ray diffraction spectroscopy (Bruker-D8 advanced diffractometer, $\text{CuK}\alpha$ line ($\lambda = 1.540598 \text{ \AA}$) radiation source), Raman Spectroscopy (Horiba Jobin- Yvon Laser Spectrometer 6400 using 514.5 nm wavelength as excitation source), scanning electron microscope (SEM, model: VP-EVO, MA-10, Carl-Zeiss, UK) and vibrating sample magnetometer (VSM, model 7304, Lakeshore Cryotronics Inc., USA).

The dye adsorption performance of MAP was studied by adding a known amount of MAP in MB aqueous solution of known concentration. The adsorbent-adsorbate mixture was shaken for 30 s and the colour of dye solution was observed. Finally the dye adsorbed adsorbent was magnetically recovered from clear aqueous phase.

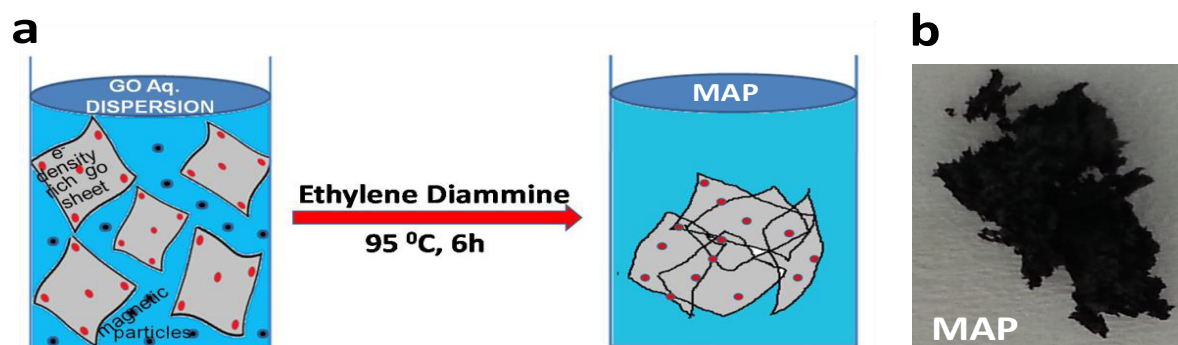


Figure 1. (a) Schematic representation of synthesis process (b) Digital photographs of MAP.

3. RESULTS AND DISCUSSION

Fourier transform infrared spectrum (FTIR) of MAP (Figure 2a) is recorded for analysis of chemical functional groups of MAP and is correlated with FTIR spectra of GO. The clear peaks around 1715 cm^{-1} and 1032 cm^{-1} along with broad hump around 3400 cm^{-1} in GO confirm the presence of carbonyl (-C=O), epoxide (-C(O)C) and hydroxyl (-OH) groups respectively, which plays a crucial role in formation of hydrogels. The FTIR of MAP revealed that the epoxy band slightly weakened, which reflect the partial removal of epoxy groups of GO during hydrothermal treatment leading the formation of aerogel with residual surface functionalities. Owing to the Lewis basicity of such functional groups, they are expected to effectively interact with dyes for efficient adsorption.

The Raman microscopic structural analysis (Figure 2b) of graphitic phase in GO and MAP shows the presence of characteristic D- and G-bands for around 1360 cm^{-1} and 1596 cm^{-1} respectively for GO which shifted to lower wavenumber for MAP i.e. 1351 cm^{-1} and 1588 cm^{-1} respectively. Further, compared to GO, in MAP there was slight increase in relative

intensity of D-band compared to G-band. Such a variation in relative position and intensity of bands compliments the FTIR observations and confirm the partial reduction of GO phase to RGO in MAP. The confirmation of reduction also comes from shifting of XRD peak from 110 for GO (Figure 2c) to 260 (Figure 2d) for MAP (Saini et al., 2016a and Moon et al., 2010), whereas incorporation of magnetic Fe_3O_4 phase was confirmed from observation of weak signature around 350 . The partial reduction ensures the residual oxygen functionalities, which is considered useful for dye adsorption whereas magnetic character provide magnetic separation ability.

The MAP is composed of randomly interconnected reduced GO (RGO) sheets (containing entrapped Fe_3O_4 nanoparticles) which were formed during the hydrothermal treatment of $\text{GO/Fe}_3\text{O}_4$ dispersion with ethylenediamine (EDA). The formed macroscopic 3D self assembled aerogel (Figure 1b) is a dark black coloured loose fluffy mass having very low density ($<50\text{ mg/cm}^3$), reflecting highly porous structure.

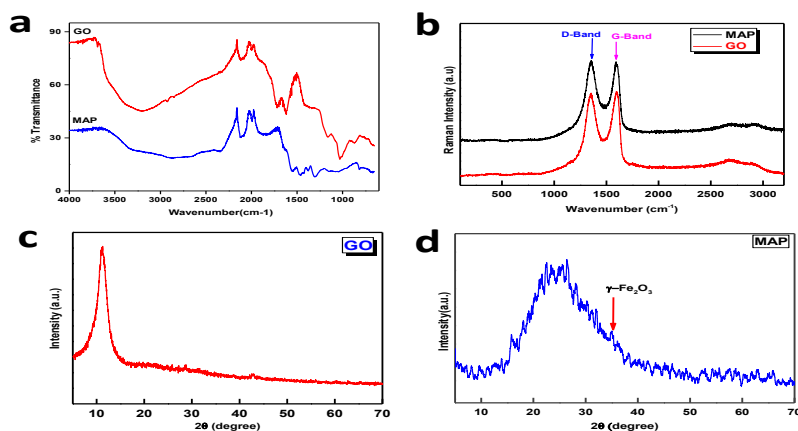


Figure 2. (a) FTIR spectra (b) Raman spectra (c, d) X-ray diffraction patterns of GO and MAP.

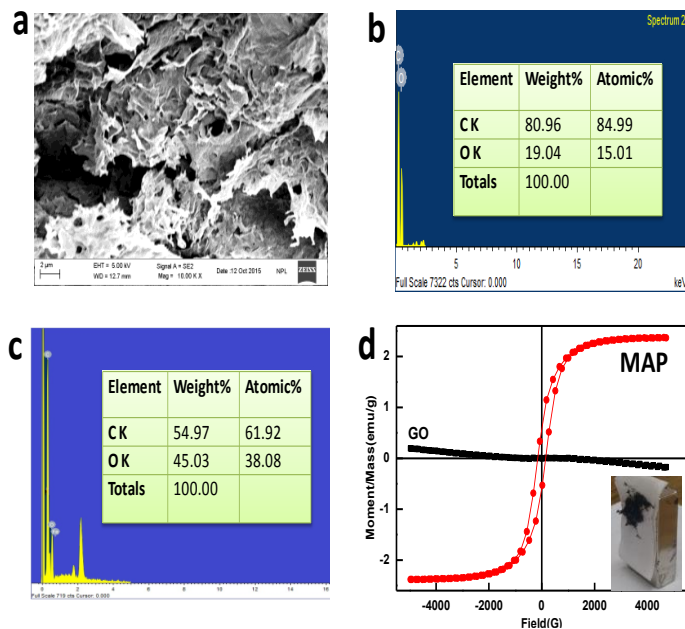


Figure 3. (a) SEM image of MAP. SEM- EDX analysis of (b) MAP and (c) GO (d) VSM plots of MAP.

The internal microstructure of MAP was investigated through Scanning electron microscopy (SEM). The SEM image of MAP is shown in Figure 3a which revealed the presence of highly porous but loosely interconnected 3D structure constituted by randomly interconnected graphitic layers. The SEM-EDX analyses of MAP (Figure 3b) and GO (Figure 3c) confirm the partial removal of oxygen functional groups during transformation of GO-magnetite dispersion to MAP. The data also revealed plenty of residual oxygen functionalities present in MAP which were responsible for high affinity towards dyes. The VSM plots (Figure 3d) of GO and MAP confirm the enhanced magnetic character of MAP which was previously absent in GO. The visual evidence of the magnetic character of MAP has also been demonstrated (inset Figure 3d) which shows the instantaneous attraction of MAP particles permanent bar magnet. Such a combination of residual surface functionalities, high porosity, low density and magnetic actuation is considered beneficial for efficient dye adsorption and facile separation of spent adsorbent particles from purified aqueous phase.

Figure 4 shows the digital images of MB adsorption on MAP surface. The adsorption studies revealed that the adsorption kinetics of dye molecules on MAP surface was very fast and the adsorption capacity of MAP was found to be 130 mg/g of adsorbent in just 30 s of adsorption process. Further, the dye adsorbed MAP has been easily separated from purified water using a magnetic bar as shown in Figure

4. This efficient and fast adsorption of MB by MAP is attributed to the very light weight, high porosity and Lewis basicity of functional groups present on the surface of MAP.

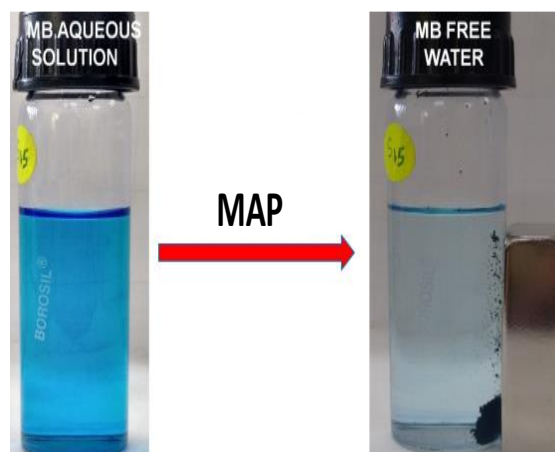


Figure 4. Digital photographs of adsorption process of MB dye on MAP.

A schematic illustration of the adsorption mechanism has been shown in Figure 5 which depicts the involvement of strong and ultrafast electrostatic interactions between positively charged dye molecules and negatively charged MAP surfaces. Nevertheless, the presence of electron rich porous architecture with magnetic character enables MAP to act as an effective and efficient adsorbent material for MB dye which can also be easily employed for large scale waste water treatment of industrial effluents containing other dyes and heavy metal ions.

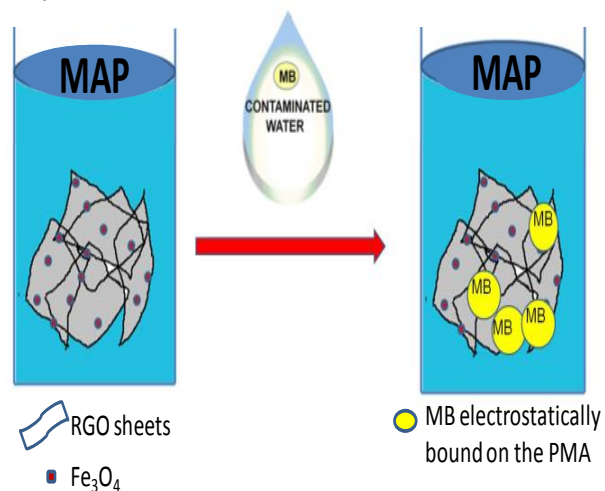


Figure 5. Schematic representation of the adsorption mechanism of MB on MAP surface.

4. CONCLUSIONS

In summary, a MAP material has been prepared by facile route involving hydrothermal treatment and subsequent freeze drying, and its MB adsorption performance was studied. The characterization of MAP reveals that the porosity and surface acidity plays a significant role in fast and efficient MB adsorption and whereas magnetic character facilitates easy recovery by magnetic separation. It is believed that besides efficient dye removal efficiency, the MAPs can be also used for treatment of other water pollutants such as heavy metal ions.

ACKNOWLEDGEMENTS

Authors are thankful to the Director, NPL for providing necessary research facilities. R.S. is thankful to UGC for Junior Research Fellowship. Authors are thankful to Mr. M. Saravanan of NPL for SEM measurements and Dr. N. Vijayan for XRD measurements. The partial financial assistance by CSIR via Young Scientist Grant and DST via Fast Track Grant for Young Scientists is duly acknowledged.

REFERENCES

- Ai, L., Li, M. and Li, L. (2011) Adsorption of methylene blue from aqueous solution with activated carbon/cobalt ferrite/alginate composite beads: Kinetics, isotherms and thermodynamics. *Journal of Chemical and Engineering Data*, 56, 3475–3483.
- Ambashta, R.D. and Sillanpää, M. (2010) Water purification using magnetic assistance: A review. *Journal of Hazardous Materials*, 180, 38–49.
- Bhatnagar, A. and Sillanpää, M. (2010) Utilization of agro-industrial and municipal waste materials as potential adsorbents for water treatment—A review. *Chemical Engineering Journal*, 157, 277–296.
- Dias, J.M., Alvim-Ferraz, M.C., Almeida, M.F., Rivera-Utrilla, J. and Sánchez-Polo, M. (2007) Waste materials for activated carbon preparation and its use in aqueous-phase treatment: A review. *Journal of Environmental Management*, 85, 833–846.
- Jiao, T., Guo, H., Zhang, Q., Peng, Q., Tang, Y., Yan, X. and Li, B. (2015) Reduced graphene oxide-based silver nanoparticle-containing composite hydrogel as highly efficient dye catalysts for wastewater treatment. *Scientific Reports*, 5, 11873.
- Hummers, W. and Offeman, R.E. (1958) Preparation of graphitic oxide. *Journal of American Chemical Society*, 80, 1339.
- Khan, W., Sharma, R. and Saini, P. (2016) Carbon nanotubes - current progress of their polymer composites, Eds. Berber, M.R. and Hafez, I.H. *InTech*, doi: 10.5772/62497.
- Khin, M.M., Nair, A. S., Babu, V.J., Murugan, R. and Ramakrishna, S. (2012) A review on nanomaterials for environmental remediation. *Energy Environmental Sciences*, 5, 8075.
- Moon, I.K., Lee, J., Ruoff, R.S. and Li, H. (2010) Reduced graphene oxide by chemical graphitization. *Nature Communications*, 1, 1–6.
- Mukherjee, R., Sharma, R., Saini, P. and De, S. (2015) Nanostructured polyaniline incorporated ultrafiltration membrane for desalination of brackish water. *Environmental Science and Water Research Technology*, 1, 893–904.
- Muthuraman, G., Teng, T.T., Leh, C.P. and Norli, I. (2009) Extraction and recovery of methylene blue from industrial wastewater using benzoic acid as an extractant. *Journal of Hazardous Materials*, 163, 363–369.
- Namasivayam, C. and Kavitha, D. (2002) Removal of Congo red from water by adsorption onto activated carbon prepared from coir pith, an agricultural solid waste. *Dyes and Pigments*, 54, 47–58.
- Pradeep, T. and Anshup. (2009) Noble metal nanoparticles for water purification: A critical review. *Thin Solid Films*, 517, 6441–6478.
- Prado, A.G.S. and Costa, L.L. (2009) Photocatalytic decoloration of malachite green dye by application of TiO₂ nanotubes. *Journal of Hazardous Materials*, 169, 297–301.
- Rafatullah, M., Sulaiman, O., Hashim, R. and Ahmad, A. (2010) Adsorption of methylene blue on low-cost adsorbents: A review. *Journal of Hazardous Materials*, 177, 70–80.
- Saini, P., Kaushik, S., Sharma, R., Chakravarty, D., Raj, R. and Sharma, J. (2016a) Excellent electromagnetic interference shielding effectiveness of chemically reduced graphitic oxide paper at 101 GHz. *The European Physical Journal B*, 89, doi:10.1140/epjb/e2016-60624-7
- Saini, P., Sharma, R. and Akodia, S. (2016b) Graphene oxide and reduced graphene oxide coated polyamide fabrics for antistatic and electrostatic charge dissipation. *World Journal of Textile Engineering and Technology*, 2, 1-5.
- Shannon, M.A., Bohn, P.W., Elimelech, M., Georgiadis, J.G., Marinas, B.J. and Mayes, A.M. (2008) Science and technology for water purification in the coming decades. *Nature*, 452, 301–310.
- Sharma, R. and Saini, P. (2016) Graphene-based composites and hybrids for water purification applications. in: Aliofkhaezai, M. Ed.; diamond and carbon composites and nanocomposites. *InTech*, Croatia, doi: 10.5772/63666.
- Sulak, M.T. and Yatmaz, H.C. (2012) Removal of textile dyes from aqueous solutions with eco-friendly biosorbent. *Desalination and Water Treatment*, 37, 169–177.
- Tan, B. (2000) Removal of dyes and industrial dye wastes by magnesium chloride. *Water Research*, 34, 597–601.
- Tripathi, S.N., Saini, P., Gupta, D. and Choudhary, V. (2013) Electrical and mechanical properties of PMMA/reduced graphene oxide nanocomposites prepared via in situ polymerization. *Journal of Materials Science*, 48, 6223–6232.